This is the Pre-Published Version.

The following publication Z. Li, W. Shi, H. Zhang and M. Hao, "Change Detection Based on Gabor Wavelet Features for Very High Resolution Remote Sensing Images," in IEEE Geoscience and Remote Sensing Letters, vol. 14, no. 5, pp. 783-787, May 2017 is available at https://doi.org/10.1109/LGRS.2017.2681198.

Change Detection Based on Gabor Wavelet Features for Very High Resolution Remote Sensing Images

Zhenxuan Li, Wenzhong Shi, Hua Zhang and Ming Hao

***Abstract*—In this letter, we propose a change detection method based on Gabor wavelet features for very high resolution (VHR) remote sensing images. First, Gabor wavelet features are extracted from two temporal VHR images to obtain spatial and contextual information. Then, the Gabor wavelet based difference measure (GWDM) is designed to generate the difference image. In GWDM, a new local similarity measure is defined, in which the Markov random field neighborhood system is incorporated to get the local relationship, and the coefficient of variation method is applied to discriminate the contributions of different features. Finally, the Fuzzy *c*-means cluster algorithm is employed to obtain the final change map. Experimental carried out on QuickBird and SPOT5 images demonstrate the effectiveness of the proposed approach.**

***Index Terms*—Change detection, Gabor wavelet, Markov random field, coefficient of variation, Fuzzy *c*-means, very high resolution, remote sensing.**

I. INTRODUCTION

Remote sensing change detection is to identify the changes occurred on the Earth surface by jointly processing multi-temporal images acquired from the same geographical area at different times [1-3]. This technique has become an attractive research topic for its various practices applications, e.g., deforestation, damage assessment, disasters monitoring and urban expansion [4]. In the past decades, a variety of change detection approaches have been developed, such as change vector analysis (CVA) [5], fuzzy *c*-means (FCM) [6], and support vector machine [7]. With the emergence of very high resolution (VHR) remote sensing image, more detailed ground information can be obtained, while increasing in the spatial resolution always leads to reduction in the spectral statistical separability among different classes. The conventional change detection methods only utilize spectral information regardless of spatial information, which is inadequate for VHR remote sensing image change detection. However, VHR remote sensing image contains abundant spatial and contextual information can help for accurate change detection.

Gabor wavelet transform is proved to be an effective method for image features extraction [8, 9]. This method adopts Gabor function as the mother wavelet, and has good characteristics of orientation and scale invariance. For the last decades, Gabor wavelets have resulted in many successful practical applications, such as image classification [10], image segmentation [11], image retrieval [12], object extraction [13] and pattern recognition [14]. Recently, Gabor wavelets have also been researched in change detection [15-17]. In [15], Gabor filter was utilized to extract the spatial and contextual features at different scales and orientations, and a novel post-classification change detection method was proposed using these information. In [16], a simple yet effective unsupervised change detection approach was designed for multi-temporal synthetic aperture radar images by jointly exploiting the robust Gabor wavelet representation and the advanced cascade clustering. In [17], the authors performed a robust principal component analysis techniques to separate irrelevant and noisy elements from Gabor responses for change detection.

Although a lot of efforts have been spent on improving the Gabor features based methods, the practical and effective method need to be developed. In previous work, the Gabor features were extracted from the difference image, which can be obtained by CVA from two temporal images. However, plenty of the spatial and contextual information presented in VHR images cannot be extracted in this way, due to much information is missed in the differencing process. Besides, the pixel-wise difference measure (i.e. CVA) is not suitable for Gabor wavelet features for their spatial correlation. Therefore, an effective difference measure based on Gabor features is proposed based on the extracted Gabor features from the original images.

In this letter, a change detection method based on Gabor wavelet features is proposed for VHR images. The main contributions consist of two parts: 1) a new Gabor based change detection procedure is designed based on the Gabor wavelet features, which were extracted from the two original temporal original VHR images; 2) A Gabor wavelet based difference

This work was supported in part by the National Natural Science Foundation of China under Grant 41331175; by a Project Funded by the Priority Academic Program Development of Jiangsu Higher Education Institutions; by the Fundamental Research Funds for the Central Universities under Grant 2015XKQY09; and by the Natural Science Foundation of Jiangsu Province under Grant BK20160248.

Z. Li, H. Zhang and M. Hao are with the School of Environment Science and Spatial Informatics, China University of Mining and Technology, Xuzhou 221116, China (e-mail: zxlicumt@126.com; zhhuamesi@gmail.com; haomingcumt@gail.com).

W. Shi is with the Department of Land Surveying and Geo-informatics, The Hong Kong Polytechnic University, Kowloon, Hong Kong (e-mail: lswzshi@polyu.edu.hk).

© 2017 IEEE. Personal use of this material is permitted. Permission from IEEE must be obtained for all other uses, in any current or future media, including reprinting/republishing this material for advertising or promotional purposes, creating new collective works, for resale or redistribution to servers or lists, or reuse of any copyrighted component of this work in other works.

measure (GWDM) is proposed, in which the spatial correlation of the Gabor features is fully considered using Markov random field (MRF) [18] neighborhood system, and the weights between different features are also taken in to account by the coefficient of variation method (CVM) [19] according to their contributions.

This letter is organized as follows. Section II describes the proposed change detection approach. Section III presents the experiments and analysis, and section IV concludes this letter.

II. CHANGE DETECTION BASED ON GABOR WAVELET FEATURES FOR VHR IMAGES

A. Problem Formulation

Supposing two co-registered and radiometrically corrected VHR remote sensing images acquired over the same geographical area at times t_1 and t_2. Let X_1 and X_2 be the two images, which have the same size of $M \times N$. As shown in Fig. 1(a) and 1(b), two corresponding simulated image chips were acquired from the original images of X_1 and X_2, respectively. The difference image generated by subtracting the two images chips was shown in Fig. 1(c).

To demonstrate the necessity of Gabor features extraction before the differencing process, a theoretical analysis is exploit as follows. As can be seen from Fig. 1, the two temporal original image chips have abundant spatial and contextual information, but the difference image has little (i.e. the area inside the dotted line in Fig. 1). A large amount of structural information was destroyed from the differencing process. As a result, many features included in the original images cannot be extracted and applied for change detection.

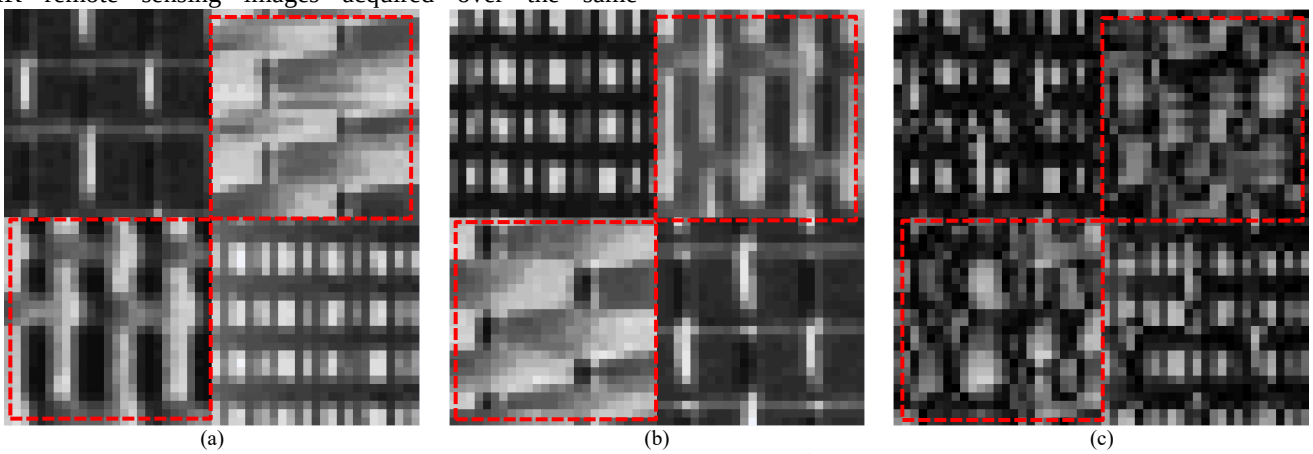

Fig. 1. (a) The simulated image chip at time t_1. (b) The simulated image chip at time t_2. (c) The difference image generated by subtracting the two image chips.

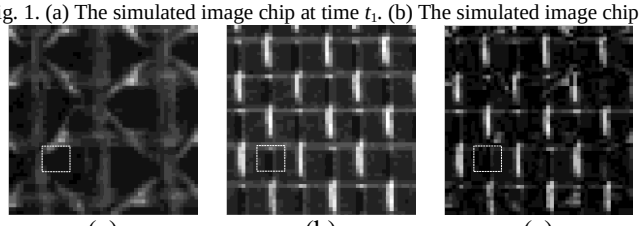

Fig. 2. (a) Gabor feature of simulated image chip at time t_1. (b) Gabor feature of simulated image chip at time t_2. (c) The difference image generated by CVA.

After the Gabor features extraction from the original images, a difference measure is needed to detect the changes based on multi features of two temporal images. Apparently, the pixel-wise difference measure (i.e. CVA) is not suitable for images including the strong spatial correlation inside the features. As shown in Fig. 2(a) and 2(b), two corresponding Gabor feature image chips were obtained and the difference image generated by CVA was shown in Fig. 2(c). Let us focus on the image regions highlighted by white boxes in Fig. 2. According to the traditional method, this region will be directly classified into unchanged class. However, this result was not completely reasonable because the two temporal feature image chips were not coincident.

To address the aforementioned problems, a novel change detection method based on Gabor wavelet features was proposed for VHR remote sensing images in this letter. As shown in Fig. 3, the proposed approach consists of three blocks as follows. First, Gabor wavelet features were extracted from two temporal VHR remote sensing images, respectively. Then, GWDM was designed to generate the difference image. Finally, FCM cluster algorithm [6] was implemented to generate the final change map. The detailed descriptions are provided in section II-B, C and D.

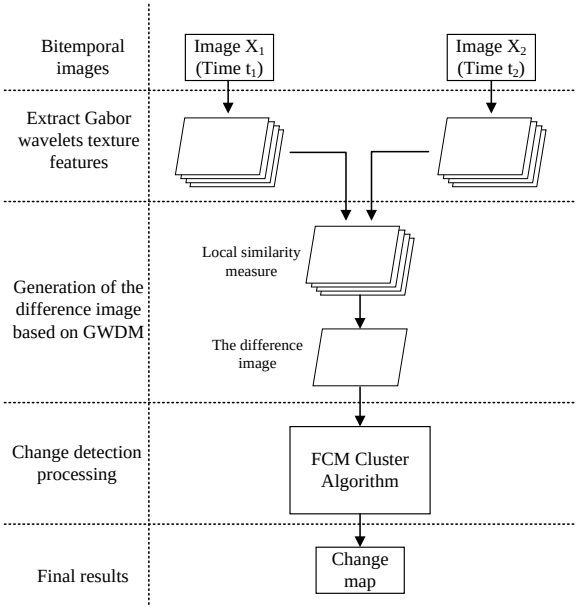

Fig. 3. Framework of the proposed change detection approach.

B. Gabor wavelet features extraction

Gabor wavelet can be considered as one of the wavelet transform, in which the Gabor function was utilized as the mother wavelet. 2-D Gabor function *g(x, y)* was written as:

$$g(x,y)=\left(\frac{1}{2\pi\sigma_x\sigma_y}\right)\exp\left[-\frac{1}{2}\left(\frac{x^2}{\sigma_x^2}+\frac{y^2}{\sigma_y^2}\right)+2\pi jWx\right], \quad (1)$$

where σ_x, σ_y, denote the standard deviation of the primary function of Gabor along the *x* axis and the *y* axis, respectively, $j=\sqrt{-1}$ and *W* denotes the frequency bandwidth of Gabor. Its Fourier transform *G(u, v)* can be presented as:

$$G(u,v)=\exp\left\{-\frac{1}{2}\left[\frac{(u-W)^2}{\sigma_u^2}+\frac{v^2}{\sigma_v^2}\right]\right\}, \quad (2)$$

where $\sigma_u=1/2\pi\sigma_x$, $\sigma_v=1/2\pi\sigma_y$. Let *g(x, y)* be the mother Gabor wavelet, then a set of self-similar Gabor filter can be generated by proper scale and rotation transformation for *g(x, y)*. The filters can be denoted as

$$g_{mn}(x,y)=a^{-m}G(x',y'),a>1,m,n=\text{integer}, \quad (3)$$

where $x'=a^{-m}(x\cos\theta+y\sin\theta)$, $y'=a^{-m}(-x\sin\theta+y\cos\theta)$, $\theta=n\pi/K$, *K* is the total number of orientations, $n\in[0, K\text{-}1]$. a^{-m} is the scale factor, $m\in[0, S\text{-}1]$, *S* is the total number of scales.

In order to decrease the redundant information among the Gabor features, the parameters of the Gabor wavelet are set as follows

$$a=(U_h/U_l)^{-\frac{1}{S-1}},\sigma_u=\frac{(a-1)U_h}{(a+1)\sqrt{2\ln 2}}$$
$$\sigma_v=\tan\left(\frac{\pi}{2k}\right)\left[U_h-2\ln\left(\frac{\sigma_u^2}{U_h}\right)\right]\left[2\ln 2-\frac{(2\ln 2)^2\sigma_u^2}{U_h^2}\right]^{-\frac{1}{2}} \quad (4)$$

where U_l and U_h denote the lower and upper center frequencies of interest.

Given an image *I(x, y)*, its 2-D Gabor wavelet transform can be defined as

$$W_{mn}(x,y)=\int I(x_1,y_1)g_{mn}^*(x-x_1,y-y_1)dx_1dy_1, \quad (5)$$

where * denotes the complex conjugate. As such, the Gabor wavelet features are extracted from the VHR remote sensing images.

C. Gabor wavelet based difference measure

After the Gabor features extraction, the GWDM is defined to generate the difference image. In GWDM, a local similarity measure $S_{mn}(t_1,t_2)$ based on the MRF neighborhood system between two temporal Gabor features is designed and it can be formulated as

$$S_{mn}(t_1,t_2)=\frac{1}{1+d_{mn}(t_1,t_2)}, \quad (6)$$

in which,

$$d_{mn}(t_1,t_2)=\sqrt{\left(\left[W_{mn}^{t_1}(u,v)-W_{mn}^{t_2}(u,v)\right]^2+\sum_{(u,v)\in\omega}\left(\frac{W_{mn}^{t_1}(u,v)-W_{mn}^{t_2}(u,v)}{h}\right)^2\right)} \quad (7)$$

where $d_{mn}(t_1,t_2)$ denotes the variation index between two temporal corresponding Gabor feature regions at the scale *m* and the orientation *n*. $W_{mn}^{t_1}(u,v)$, $W_{mn}^{t_2}(u,v)$ present Gabor wavelet features at times t_1 and t_2, respectively. *(u,v)* denotes the position of the target pixel in the image. ω means MRF neighborhood system centered at the target pixel, as shown in Fig. 4(a). *h* denotes the distance between the target pixel and its neighborhood pixels as shown in Fig. 4(b).

(u-1,v-1)	(u,v-1)	(u+1,v-1)
(u-1,v+1)	(u,v)	(u+1,v+1)
(u+1,v+1)	(u,v+1)	(u+1,v+1)

(a)

$\sqrt{2}$	1	$\sqrt{2}$
1	(u,v)	1
$\sqrt{2}$	1	$\sqrt{2}$

(b)

Fig. 4. (a) Neighborhood system centered at (*u, v*). (b) Distance between the center pixel (*u, v*) and its neighborhoods.

Using the local similarity measure, the similarity images at each scale and orientation are generated from the two temporal Gabor wavelet features. In order to display the contributions of different Gabor features, a weight determination method, namely CVM, is utilized in this letter. In CVM, the weights of each features can be calculated as

$$W_{mn}=\frac{V_{mn}}{\sum_m^S\sum_n^K V_{mn}},\text{and } V_{mn}=\frac{\sigma_{mn}}{\mu_{mn}} \quad (8)$$

where V_{mn} presents the coefficient of variation of the Gabor feature at the scale *m* and the orientation *n*, μ_{mn} and σ_{mn} are the mean value and the standard deviation of this feature, respectively.

Then, the difference image can be generated as

$$D(t_1,t_2)=\sum_m^S\sum_n^K\frac{W_{mn}}{S_{mn}(t_1,t_2)}. \quad (9)$$

In this way, the difference image is obtained using GWDM.

D. Change detection

Once the difference image has been generated, the change detection processing is needed to classify the changed pixels and unchanged pixels. In this letter, the FCM cluster algorithm is utilized to generate the final change map.

Supposing $X=\{x_1, x_2,\ldots, x_n\}$ is the difference image, in which $n=M\times N$, and *c* is the number of clusters. Then, the membership probability of the pixel x_j in the difference image belonging to the *i*th cluster can be written as

$$u_{ij}\in[0,1]\left(\sum_{i=1}^c u_{ij}=1(j=1,2,\cdots,n)\right) \quad (10)$$

Using the membership probability, the objective function of FCM is presented as

$$J(U,c_1,c_2,\cdots,c_c)=\sum_{i=1}^c\sum_j^n u_{ij}^m d_{ij}^2 \quad (11)$$

where $U=[u_{ij}]$ is the membership probability matrix of *X*, and c_i denotes the centre of the *i*th cluster. $d_{ij}=\|c_i-x_j\|$ denotes the Euclidean distance between the *i*th cluster and the *j*th pixel. $m\in[1,\infty]$ denotes the weighting exponent. By minimizing this function, the membership probability can be obtained. To reach the minimization of the objective function, an iteration process is developed as follows

$$c_i = \frac{\sum_{j=1}^{n} u_{ij}^{m} x_j}{\sum_{j=1}^{n} u_{ij}^{m}} \tag{12}$$

$$u_{ij} = \frac{1}{\sum_{k=1}^{c} \left(\frac{d_{ij}}{d_{kj}} \right)^{2/(m-1)}} \tag{13}$$

The iteration process is stopped when a predefined maximum iterations are reached or the difference of clusters between adjacent two iterations is less than a predefined minimum threshold. In this way, the final change map is generated.

III. EXPERIMENTS AND ANALYSIS

In order to evaluate the performance of the proposed approach, two temporal VHR remote sensing images were used. Three indices in terms of experimental result and the ground truth were adopted for quantitative evaluation, such as false alarm rate P_F, missed detection rate P_M and total error rate P_T. Specifically, $P_F = N_f/N_u$, where N_f is the number of changed pixels in the change detection result which were classified as the unchanged class in the ground truth image, and N_u is the total number of unchanged pixels counted in the ground truth image. $P_M = N_m/N_c$, where N_m is the number of unchanged pixels in the change detection result which were classified as the changed class in the ground truth image, and N_c is the total number of changed pixels counted in the ground truth image. $P_T = (N_m+N_f)/(N_c+N_u)$.

To demonstrate the performance of the proposed method, comparisons between the proposed algorithm and the traditional change detection algorithms, i.e., Expectation Maximization based algorithm (EM) and FCM algorithm, were implemented. Additionally, to highlight the effectiveness of Gabor features, a variant of the proposed approach by replacing the FCM with EM, referred to as Gabor-EM, was developed.

A. Description of the Data sets and Experimental Setup

The first data set contains two VHR images of size 470×548 pixels acquired by the QuickBird satellite collected on the city of Wuhan of China on April 1, 2002 and July 16, 2009, as shown in Fig. 5(a) and (b). The spatial resolution of this image is 2.4m. The main land covers are water, grass, road and building. The ground truth image of the data set is shown in Fig. 5 (c), which was generated by visual interpretation. The second data set (600×600) was obtained by Satellite Probatoire d'Observation de la Terre 5 (SPOT5) collected on the city of Tianjin of China on April 24, 2008 and February 23, 2009, respectively, and they were generated by fusing panchromatic and multispectral images. The spatial resolution of this data set is 2.5m. Its main land types are farmland, road and building. The ground truth of the change detection map shown in Fig. 6(c) was manually created based on the input images shown in Fig. 6(a) and (b).

(a) (b) (c)

Fig. 5. QuickBird data set. (a) QuickBird image from 2002. (b) QuickBird image from 2009. (c) Ground truth image.

(a) (b) (c)

Fig. 6. SPOT5 data set. (a) SPOT5 image from 2008. (b) SPOT5 image from 2009. (c) Ground truth image.

In the two experiments, the relevant parameters are set as follows. In Gabor wavelet features extraction, some parameters are implemented using the default parameters provided in, such as U_l =0.05, U_h =0.4, S =4, and K =6. The window size of Gabor filter is chosen based on experiences. The sizes in the QuickBird experiment and in the SPOT5 experiment are 5 and 9, respectively. In FCM cluster algorithm, the initial membership probability is randomly generated with uniformly distributed values in (0, 1), c=2, m=2, ε=1e-5, and the maximum iterations is 200.

B. Experimental Results and Analysis

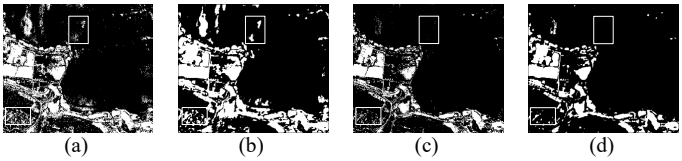

(a) (b) (c) (d)

Fig. 7. Change detection results for the different methods with the QuickBird imagery. (a) EM. (b) FCM. (c) Gabor-EM. (d) Proposed method.

TABLE I
COMPARISIONS OF THE DIFFERENT CHANGE DETECTION APPROACHES WITH THE QUICKBIRD IMAGE

Method	False Alarms		Missed Detections		Total Errors	
	pixels	P_F (%)	pixels	P_M (%)	pixels	P_T (%)
EM	28598	12.63	4925	15.78	33523	13.02
FCM	32127	14.19	3465	11.11	35592	13.82
Gabor-EM	11295	4.99	8011	25.68	19306	7.5
Proposed	10780	4.76	6762	21.67	17542	6.81

Fig. 7(a)-(d) and 8(a)-(d) show the change detection results by the use of EM, FCM, Gabor-EM and the proposed method for the QuickBird and SPOT5 images, respectively. The visual comparisons of the four change detection approaches can generally present the performances of different change detection methods. Compared with the ground truth images in Fig. 5(c) and 6(c), Gabor-EM and our proposed method have better visual change detection results and have fewer error pixels. Compared with the traditional change detection

methods shown in Fig. 7(a), (b) and 8(a), (b), some of the improved change detection areas using the Gabor based approaches, as shown in Fig. 7(c), (d) and 8(c), (d), are highlighted by white boxes. The results indicate that the spatial contextual information generated by the Gabor wavelet features can effectively decrease the false alarms rate and improve the final change detection results.

Table I and table II show the P_F, P_M and P_T values of the four change detection approaches from the QuickBird and SPOT5 data sets. As shown in Table I and table II, the Gabor-EM and our proposed method outperform EM and FCM methods in change detection performance. Specifically, for the QuickBird data set, the total error rates of Gabor-EM and our proposed method were improved by 5.52% and 7.01% than EM and FCM, respectively. For the SPOT5 data set, the total error rates of Gabor-EM and our proposed method respectively were improved by 3.01% and 4.06% than EM and FCM. In addition, the proposed method provides a better performance than Gabor-EM from the two data sets. This indicates that the proposed cascade scheme is helpful to discriminate the changed and unchanged pixels, and works well than the traditional methods. Meanwhile, the quantitative comparison results is coincident with the visual comparison results.

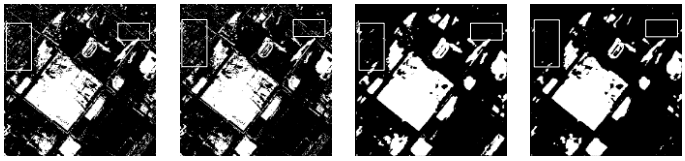

(a) (b) (c) (d)

Fig. 8. Change detection results for the different methods with the SPOT5 imagery. (a) EM. (b) FCM. (c) Gabor-EM. (d) Proposed method.

TABLE II
COMPARISIONS OF THE DIFFERENT CHANGE DETECTION APPROACHES WITH THE SPOT5 IMAGE

Method	False Alarms		Miss Detections		Total Errors	
	pixels	P_F (%)	pixels	P_M (%)	pixels	P_T (%)
EM	19400	7.24	19388	21.09	38788	10.77
FCM	17953	6.7	20155	21.92	38108	10.59
Gabor-EM	14666	5.47	13273	14.44	27939	7.76
Proposed	5520	2.06	17993	19.57	23513	6.53

IV. CONCLUSION

A novel change detection technique based on Gabor wavelet features has been proposed and implemented for VHR remote sensing images in this letter. The proposed algorithm extracts Gabor wavelet features from two temporal VHR images before the differencing process to obtain the spatial and contextual information. The GWDM based on MRF and CVM are then proposed and used to generate the difference image. At last, FCM cluster algorithm is applied to obtain the final change map. The effectiveness of the proposed approach is evaluated by QuickBird and SPOT5 images and the results show that the proposed method has the ability to provide better change detection results for VHR images than the traditional change detection methods. Future work will be devoted to the feature selection and the automatic determination of the parameters.

REFERENCES

[1] L. Bruzzone, and F. Bovolo, "A Novel Framework for the Design of Change-Detection Systems for Very-High-Resolution Remote Sensing Images," *Proceedings of the IEEE*, vol. 101, no. 3, pp. 609-630, Mar, 2013.

[2] D. L. C. author, P. Mausel, E. Brondízio *et al.*, "Change detection techniques," *International Journal of Remote Sensing*, vol. 25, no. 12, pp. 2365-2401, 2004.

[3] A. P. Tewkesbury, A. J. Comber, N. J. Tate *et al.*, "A critical synthesis of remotely sensed optical image change detection techniques," *Remote Sensing of Environment*, vol. 160, pp. 1-14, 2015.

[4] M. Hussain, D. Chen, A. Cheng *et al.*, "Change detection from remotely sensed images: From pixel-based to object-based approaches," *ISPRS Journal of Photogrammetry and Remote Sensing*, vol. 80, pp. 91-106, 2013.

[5] Z. Yetgin, "Unsupervised change detection of satellite images using local gradual descent," *IEEE Transactions on Geoscience and Remote Sensing*, vol. 50, no. 5, pp. 1919-1929, 2012.

[6] A. Ghosh, N. S. Mishra, and S. Ghosh, "Fuzzy clustering algorithms for unsupervised change detection in remote sensing images," *Information Sciences*, vol. 181, no. 4, pp. 699-715, 2011.

[7] F. Bovolo, L. Bruzzone, and M. Marconcini, "A novel approach to unsupervised change detection based on a semisupervised SVM and a similarity measure," *IEEE Transactions on Geoscience and Remote Sensing*, vol. 46, no. 7, pp. 2070-2082, 2008.

[8] J. Beck, A. Sutter, and R. Ivry, "Spatial frequency channels and perceptual grouping in texture segregation *," *Computer Vision Graphics & Image Processing*, vol. 37, no. 2, pp. 299-325, 1987.

[9] J. G. Daugman, "Uncertainty relation for resolution in space."

[10] R. Manthalkar, P. K. Biswas, and B. N. Chatterji, "Rotation invariant texture classification using even symmetric Gabor filters," *Pattern Recognition Letters*, vol. 24, no. 12, pp. 2061-2068, 2003.

[11] N. Senin, R. K. Leach, S. Pini *et al.*, "Texture-based segmentation with Gabor filters, wavelet and pyramid decompositions for extracting individual surface features from areal surface topography maps," *Measurement Science and Technology*, vol. 26, no. 9, pp. 095405, 2015.

[12] B. S. Manjunath, and W.-Y. Ma, "Texture features for browsing and retrieval of image data," *IEEE Transactions on pattern analysis and machine intelligence*, vol. 18, no. 8, pp. 837-842, 1996.

[13] H. Jin, Y. Feng, and M. Li, "Towards an automatic system for road lane marking extraction in large-scale aerial images acquired over rural areas by hierarchical image analysis and Gabor filter," *International journal of remote sensing*, vol. 33, no. 9, pp. 2747-2769, 2012.

[14] L. Shen, and L. Bai, "A review on Gabor wavelets for face recognition," *Pattern analysis and applications*, vol. 9, no. 2-3, pp. 273-292, 2006.

[15] G. Campsvalls, L. Gomezchova, J. Muñozmari *et al.*, "Multitemporal image classification and change detection with kernels," *Proceedings of SPIE - The International Society for Optical Engineering*, vol. 256, no. 256, pp. 355-364, 2006.

[16] H.-C. Li, T. Celik, N. Longbotham *et al.*, "Gabor feature based unsupervised change detection of multitemporal SAR images based on two-level clustering," *IEEE Geoscience and Remote Sensing Letters*, vol. 12, no. 12, pp. 2458-2462, 2015.

[17] M. Gong, Y. Li, L. Jiao *et al.*, "SAR change detection based on intensity and texture changes," *ISPRS Journal of Photogrammetry and Remote Sensing*, vol. 93, pp. 123-135, 2014.

[18] L. Bruzzone, and D. F. Prieto, "Automatic analysis of the difference image for unsupervised change detection," *IEEE Transactions on Geoscience & Remote Sensing*, vol. 38, no. 3, pp. 1171-1182, 2000.

[19] S. T. Liu, "A mathematical programming approach to sample coefficient of variation with interval-valued observations," *TOP*, pp. 1-18, 2015.